

Article

Effect of SiO₂ Addition in Pack Aluminizing Mixture on Phase Evolution of Si-Modified Intermetallic Layers on IN800HT Alloys

Nattapong Nanta^a, Patama Visuttiptikul, and Sirichai Leelachao^{b,*}

Department of Metallurgical Engineering, Faculty of Engineering, Chulalongkorn University, Phayathai Road, Bangkok, 10330, Thailand

E-mail: ^a6170162221@student.chula.ac.th, ^{b,*}sirichai.l@chula.ac.th (Corresponding author)

Abstract. Effect of SiO₂ addition on aluminides formation in a single-step high-activity pack aluminization on Incoloy 800HT is studied. SiO₂ powder was added into pack aluminizing mixture at different theoretical ratios of the reduced Si and the remained Al, i.e. Si/(Si+Al), in range of 0-37.5 at.%. Aluminization was carried out at 1,000°C for 4 h. Microstructures, chemical compositions and phase evolution of the coatings were examined using scanning electron microscope (SEM), energy dispersive spectroscope (EDS) and X-ray diffractometer (XRD). For the undoped condition, the coatings showed three layers: (i) an outer layer as a mixture of various Al-rich intermetallics, (ii) a hyperstoichiometric β -(Fe,Ni)Al middle layer and (iii) an interdiffusion zone; it implies the formation is governed by Al inward diffusion. Although aluminides of the Si-doped specimens still showed three-layers structure, low Al content intermetallic prevailed in the outer layer while a thickness significantly decreased with higher SiO₂ content. Silicon was found either as the dissolved Si in aluminide coatings and Si segregation at the interdiffusion layer or as separated domains in β -(Fe,Ni)Al layer with restricted concentration. The results emphasize a possibility of Al-Si co-deposited single-step aluminization using SiO₂ as silicon source along with a reduction in the thermodynamic diffusing Al activity.

Keywords: Aluminizing, co-deposition, high-temperature coatings.

ENGINEERING JOURNAL Volume 26 Issue 4

Received 15 September 2021

Accepted 24 March 2022

Published 30 April 2022

Online at <https://engj.org/>

DOI:10.4186/ej.2022.26.4.1

1. Introduction

Superalloys are widely used in petrochemical heat exchangers, power plants or aviation industries where the service temperature is significantly high. Incoloy 800HT is an iron-based superalloy which exhibits good creep resistance, high rupture strength and a satisfactory high-temperature oxidation resistance due to their Cr_2O_3 protective scale [1]. The alloy is therefore used in power plants or petrochemical heat exchangers as materials for boilers, superheaters and reheaters [2, 3]. Nonetheless, a chromia scale deteriorates into a volatile CrO_3 when it is exposed to a temperature above 900°C [4, 5]. Another volatile $\text{CrO}_2(\text{OH})_2$ can also be formed by a reaction between Cr_2O_3 with a humid environment; it causes an insufficient of Cr and produces a thick Fe-Cr oxide scale with an inferior protectiveness [5]. Among several oxide formers, an alumina is remarkably stable at high temperature more than 900°C and volatilization rate in steam is lower as comparing with Cr_2O_3 [5]. Aluminization is simple yet effective surface modification of metallic alloys by a formation of intermetallics, so-called metallic aluminides, as the Al-rich sources, providing a protective Al_2O_3 scale during services. Metallic aluminides can be prepared by several methods such as pack aluminizing, slurry aluminizing, hot-dip aluminizing and chemical vapor deposition aluminizing (CVD) [6]. Among these methods, a pack aluminizing is advantageous because it can produce thick and continuous metallic aluminide layers [7-10]. For pack aluminizing, chemical compositions, mechanical toughness and protectiveness of the intermetallics are governed by diffusions of Al and metallic elements from the substrates. For pure Ni or Ni-base alloys, although a relative brittle Al-rich $\delta\text{-Ni}_2\text{Al}_3$ aluminide can be eliminated by a post heat treatment or high-temperature low-activity (HTLA) aluminization [11, 12], an inconvenience and a formation of Kirkendall's voids are still their disadvantage, respectively. Since Fe and Ni can form intermetallics with Al which have different properties, a phase existence of the aluminized layers must be taken into consideration, especially for Fe-base superalloys.

A modified aluminization by co-deposition of minor active elements such as reactive elements (REs), Si and Cr have been studied and developed in order to further improve oxidation resistance of aluminide coatings. The improvements are suggested to be due to (i) a selective oxidation of elements forming the protective scale, (ii) a reduction of scale growth rate at elevated temperature and (iii) an enhanced adherence of oxide scale on intermetallic coatings [13-16]. Co-deposition of Al and minor elements using pure metallic powders were reported to be extremely difficult because of a large difference in the standard Gibbs energies of formation for each metal halides [17].

A co-deposition of silicon with a single step high-activity pack aluminizing using both pure Al and Si as elemental sources has been investigated in [14, 18, 19]. It was reported that aluminide layer is formed by Al inward diffusion and consisted of Al-rich intermetallics due to

high Al activity. Therefore, any approach that reduces Al activity is suggested to pronounce a formation of stoichiometric aluminides, i.e. $\beta\text{-NiAl}$ or $\beta\text{-FeAl}$, with desirable high ductility and melting temperature. Expensive masteralloy had been utilized as elemental sources for reducing Al activity. [20] A co-deposition single-step high-activity pack aluminizing using SiO_2 and Cr_2O_3 as the minor elements source was conducted on low carbon steel and low alloy steel [21, 22]. SiO_2 and Cr_2O_3 can be reduced by a presence of metallic Al since Al_2O_3 is thermodynamically stable as compared to SiO_2 and Cr_2O_3 [23], resulting in extracted elemental Si or Cr which further react with activator and form their metal-chloride gaseous species. A consumption of Al powders by the mentioned reactions leads to a favorable reduction in Al activity [21, 22, 24]. Surface Al concentration on the aluminized layers on low carbon steels was found to decrease with increasing content of SiO_2 in the pack mixture with the saturated Si concentration around 4.5 wt.% [21]. The influence of SiO_2 on the growth of intermetallics produced by pack aluminization has not, however, gained research attention recently.

Since both Ni and Fe are energetically favorable to form aluminide compounds [25], an investigation on the effect of SiO_2 content on phase evolution of the Si-modified aluminides on Incoloy 800HT substrate in which Ni and Fe concentrations are comparable enables the process development which produces stoichiometric aluminides incorporated with alloying element-of-interest without additional heat treatment, especially for Fe-based alloys with high Ni content that widely used in industries suffering high-temperature oxidation. In the study, microstructures and chemical compositions of aluminide coatings prepared using different SiO_2 contents in the pack mixture powder were examined and the phase evolution was discussed.

Table 1. Nominal composition of Incoloy 800HT [1].

Element	wt.%
Fe	Balance
Cr	19.00-23.00
Ni	30.00-35.00
C	0.06-0.10
Al	0.25-0.60
Ti	0.25-0.60
Al + Ti	0.85-1.20

2. Experimental Procedure

Incoloy 800HT plate whose chemical composition is listed in Table 1 were cut with the dimension $10 \times 10 \times 3$ mm³. Substrates were polished with a 600-grit sand paper and then ultrasonically cleaned prior to an aluminization. Pack aluminizing mixture consisted of the AR-graded Al powder (Himedia, India), the AR-graded NH_4Cl activator (Kemaus, Australia), the AR-graded fumed SiO_2 powder (Kemaus, Australia) and a commercially pure Al_2O_3

powder as an inert filler. The pack mixture was weighed according to the compositions listed in Table 2. A detail on calculation for component contents is given in Appendix. The powders were mixed thoroughly a zip-lock bag containing ZrO₂ balls for 5 min. Refractory alumina crucibles were separately used as a retort for each pack composition. Incoloy 800HT substrates were submerged in the pack powder while an additional Al₂O₃ powder was filled up the crucible before sealing an alumina lid with an air-dry refractory cement. Aluminization was conducted in a quartz tube furnace purged with an industrial Ar gas at a rate of 3 L/min as the following steps: (i) a moisture-removal at 100°C for 5 min, (ii) an aluminizing period at 1,000°C for 4 h with a heating rate of 5 min/°C and (iii) a furnace cooling where Ar gas was kept being supplied during cooling down to 600°C to prevent the unexpected oxidation. Cross sections of the aluminized specimens were observed using a Hitachi SU3500 scanning electron

microscope (SEM); the equipped HORIBA X-MaxN Silicon Drift X-Ray Detector (SDD) 20 mm² energy dispersive spectroscope (EDS) was used for chemical analyses. Phase identifications of the aluminized layer was examined by a BRUKER D8 DISCOVER X-ray diffractometer (XRD) using Cu-K α line with a fixed incident angle of 5° and a scanning speed of 2°/min. Sequential polishing with specified thicknesses was performed to reveal each aluminized layer where a time gap between the polishing and the XRD measurement was about 1 h. ICSD of the reference patterns used in the study are as follow: FeNiAl₅ (#00-047-1183), Fe₂Al₅ (#00-047-1435), Ni₂Al₃ (#00-014-0648), FeAl (#00-045-0983), NiAl (#00-044-1188), Fe₄Al₁₃ (#00-050-0797) and (Cr,Fe)₅Al₈ (#00-051-0960).

Table 2. Pack compositions used in the study. The nominal ratio was calculated based on the reaction: $4Al + 3SiO_2 = 2Al_2O_3 + 3Si$.

Sample		Al (wt%)	SiO ₂ (wt%)	NH ₄ Cl(wt%)	Al ₂ O ₃ (wt%)
Name	Si/(Si+Al) ratio (at%)				
Al-0Si	0	10.00	0.00	2.00	88.00
Al-12.5Si	12.5	10.00	2.67	2.00	85.33
Al-25.0Si	25.0	10.00	5.14	2.00	82.86
Al-37.5Si	37.5	10.00	7.43	2.00	80.57

Table 3. Chemical composition of coating layer from EDS point analyses. Reference ternary phase diagrams are cited in the square bracket.

Sample	Spectrum point	Elements (at%)						Expected phases
		Al	Fe	Ni	Cr	Si	Ti	
Undoped	1	76.30	13.22	6.27	4.11	-	0.1	Fe ₄ Al ₁₃ [15-17]
	2	72.80	11.11	10.15	5.92	-	-	τ_2 -Fe ₃ NiAl ₁₀ [15-17]
	3	53.63	22.78	13.90	9.12	-	0.5	β -(Fe,Ni)Al [15]
Al-12.5Si	1	59.65	2.79	35.87	0.94	0.75	-	Ni ₂ Al ₃ [15]
	2	69.60	16.06	7.17	5.63	1.54	-	τ_2 -Fe ₃ NiAl ₁₀ [15-17]
	3	52.52	23.94	13.69	8.83	1.03	-	β -(Fe,Ni)Al [15]
	4	52.89	23.00	14.71	8.57	0.83	-	β -(Fe,Ni)Al [15]
	5	57.65	18.62	0.99	20.66	2.08	-	(Cr,Fe) ₅ Al ₈ [14]
Al-25.0Si	1	68.47	16.91	6.53	5.73	2.40	-	τ_2 -Fe ₃ NiAl ₁₀ [15-17]
	2	53.45	17.90	8.36	14.96	2.42	2.9	β -(Fe,Ni)Al [15]
	3	56.51	16.24	1.33	22.23	3.67	-	(Cr,Fe) ₅ Al ₈ [14]
Al-37.5Si	1	67.74	16.99	6.67	6.10	2.51	-	τ_2 -Fe ₃ NiAl ₁₀ [15-17]
	2	52.02	22.73	14.62	8.95	1.68	-	β -(Fe,Ni)Al [15]

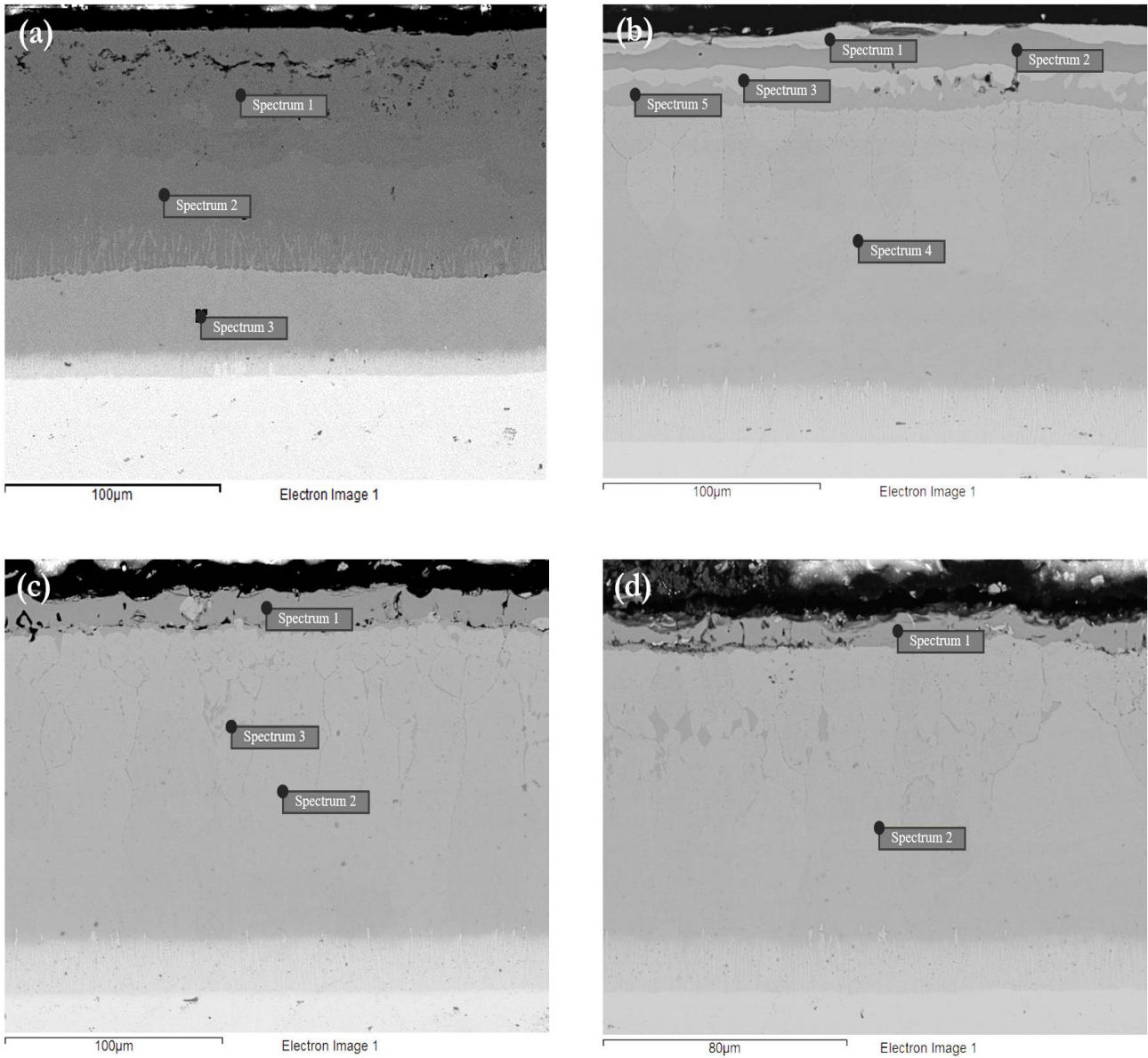


Fig. 1. Back-scattered SEM images of aluminide coating layers obtained from (a) undoped, (b) Al-12.5Si, (c) Al-25.0Si and (d) Al-37.5Si.

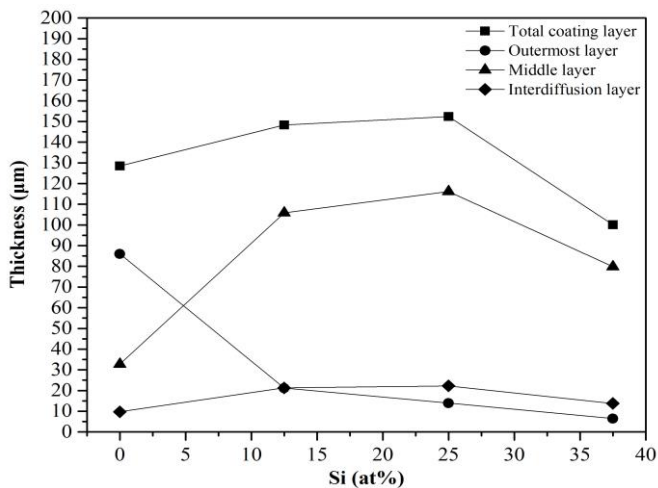


Fig. 2. Thickness of aluminide coating layers.

3. Results and Discussion

3.1. Aluminizing on IN800HT

For the undoped aluminizing, the cross-sectional images of the obtained layers with corresponding EDS locations are displayed in Fig. 1(a) whose quantitative analyses are listed in Table 3. The coating consisted of three layers with clear boundaries whose thicknesses are $86.05 \pm 1.73 \mu\text{m}$, $32.74 \pm 1.60 \mu\text{m}$ and $9.73 \pm 1.92 \mu\text{m}$, respectively. Two sub-layers in the outer layer were observed (spectrum 1 and 2). According to EDS results, they exhibited a different ratio of Fe:Ni whereas a concentration of Al is high and nearly constant. Figure 3 showed XRD patterns of the coatings at different positions. The results revealed the outer layer (0-60 μm

depth) are a mixture of Al-rich iron aluminides, i.e. $\text{Fe}_4\text{Al}_{13}$, Fe_2Al_5 and $\tau_2\text{-Fe}_3\text{NiAl}_{10}$. Peaks of Cr_5Al_8 are likely to be attributed to $(\text{Cr,Fe})_5\text{Al}_8$ [26]. According to a Fe-Ni-Al diagram [27-29], an emergence of Ni_2Al_3 and $\tau_2\text{-Fe}_3\text{NiAl}_{10}$

in the inner region was due to a limited solubility of Ni in Fe_2Al_5 than which in $\text{Fe}_4\text{Al}_{13}$.

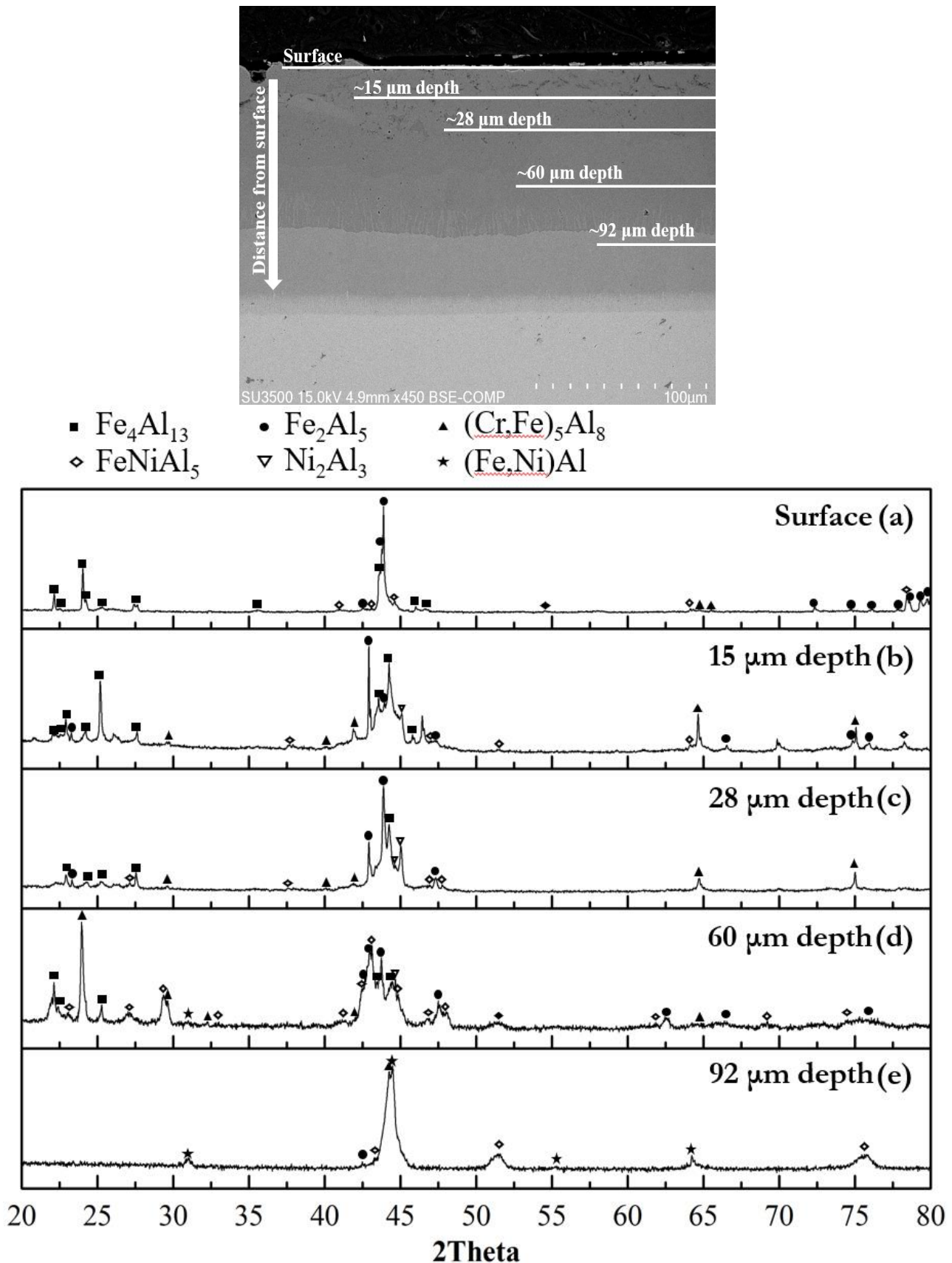


Fig. 3. XRD spectra from various depths from the surface of the undoped specimen.

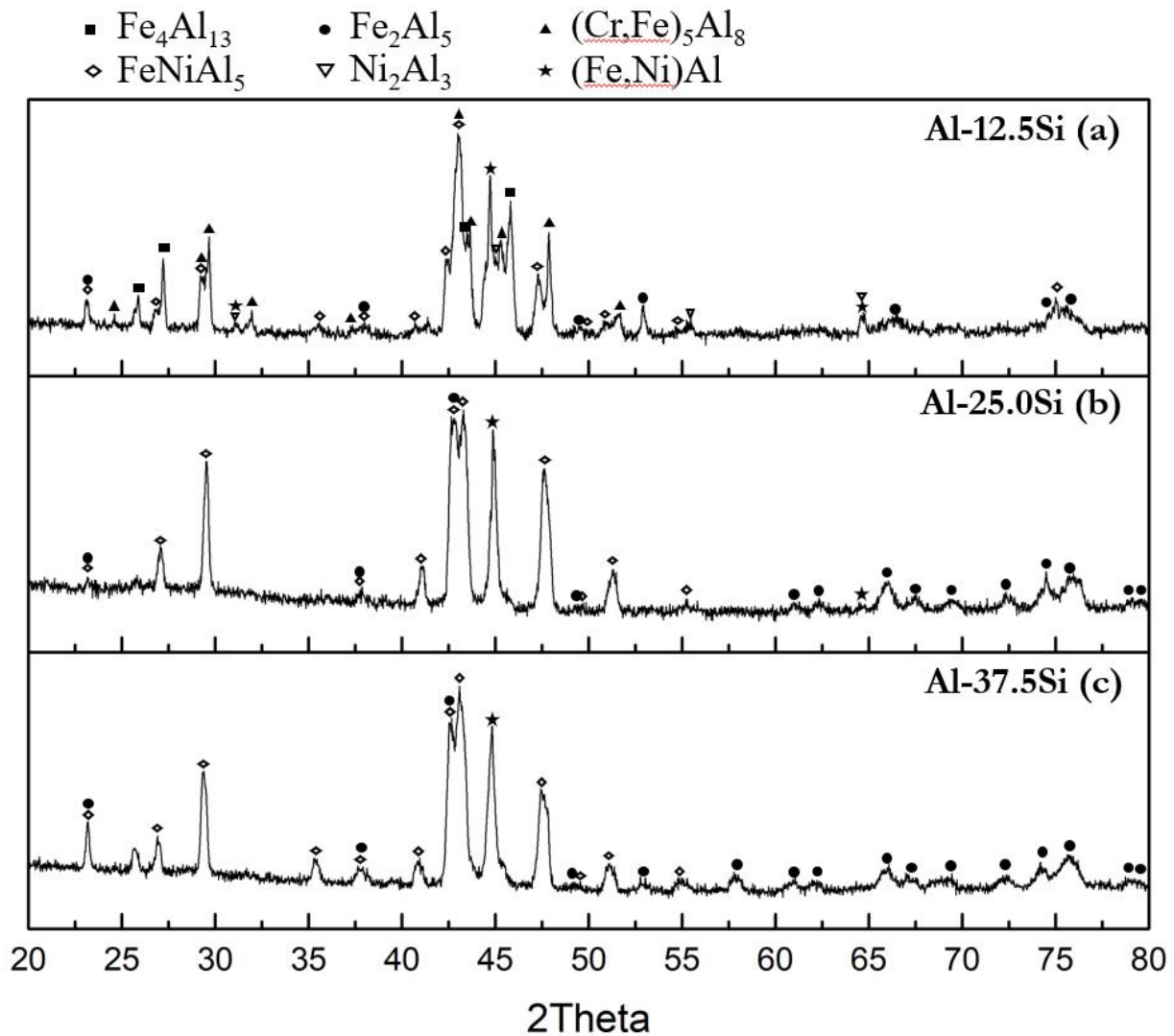


Fig. 4. XRD spectra on surface of Si-doped specimens.

The middle layer was assigned to be hyperstoichiometric β -(Fe,Ni)Al as indicated by its strong peaks at 92 μm position (Fig. 3(e)) and EDS analysis (Spectrum 3 in Fig.1(a)). At the interface between outer layer and middle layer, a formation of chromium aluminides might be due to the rejected Cr as its solubility in Fe_2Al_5 and $\tau_2\text{-Fe}_3\text{NiAl}_{10}$ is lower than that in hyperstoichiometric β -(Fe,Ni)Al [26, 30].

Regarding to the results, an aluminization is initially governed by an inward diffusion of aluminium, resulting in Al-rich intermetallics. Formation of Al-rich iron aluminides is due to a low concentration of nickel in IN800HT; this phenomenon was reported in the aluminized higher Ni-content IN825 alloy [31]. Meanwhile, an outward diffusion of Ni from the substrate produces the interdiffusion zone (IDZ) layer [8, 24, 32]. The layer of Fe_xAl_y adjacent to the IDZ is therefore enriched with Ni, allowing a hyperstoichiometric β -(Fe,Ni)Al to be formed [27-29] and grew outwardly. Microstructures are identical to those subjected to a single-step high-activity aluminizing using pure Al powder [8, 24, 32].

3.2. Influence of Addition SiO_2 on Aluminizing

SiO_2 powder was added into the pack with different concentrations: 12.5 at.%, 25.0 at.% and 37.5 at.% . The ratio of Si/(Si+Al) was calculated based on the reduced Si and the remaining Al from the following reaction: $4\text{Al} + 3\text{SiO}_2 = 2\text{Al}_2\text{O}_3 + 3\text{Si}$. Microstructures of the Al-12.5Si, the Al-25.0Si and Al-37.5Si are illustrated as Fig. 1(b)-(d), respectively. A triple-layered structure was still obtained, while the middle layer of all conditions is β -(Fe,Ni)Al, among 3 doping conditions. The EDS and XRD results (Table 3 and Fig. 4(a)) indicated that outer region of Al-12.5Si specimen exhibits a peculiar structure consisting of Ni_2Al_3 (spectrum 1), $\tau_2\text{-Fe}_3\text{NiAl}_{10}$ (spectrum 2), β -(Fe,Ni)Al (spectrum 3) and $(\text{Cr,Fe})_5\text{Al}_8$ (spectrum 5). This might be due to competitive diffusions of each species. Meanwhile, the outer layer Al-25.0Si and Al-37.5Si specimens consist of $\tau_2\text{-Fe}_3\text{NiAl}_{10}$. As the mentioned EDS and XRD results, it can conclude that Al content at surface of aluminide coating decreased. In aspect of thickness, the middle β -(Fe,Ni)Al layer became the thickest component

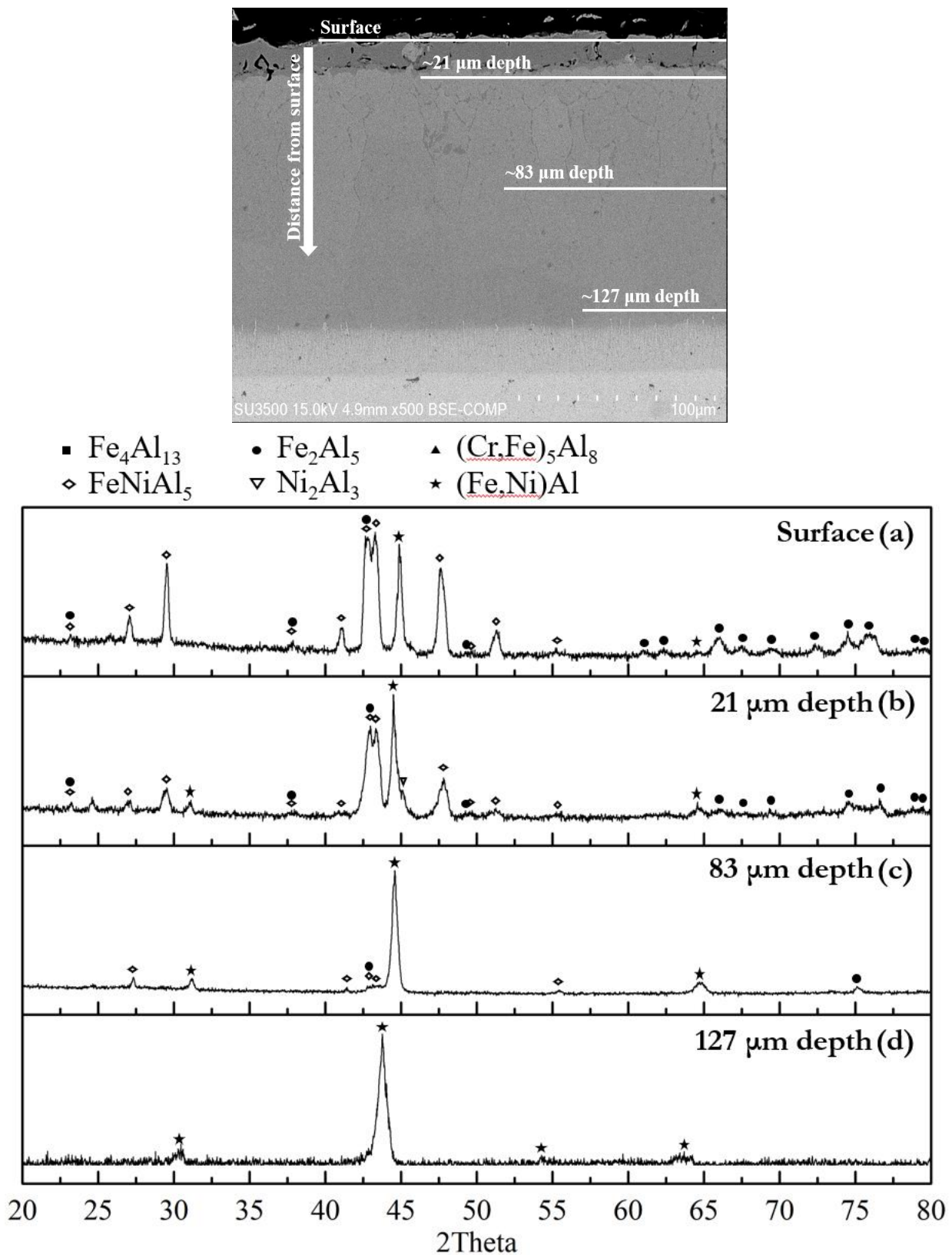


Fig. 5. XRD spectra from various depths from the surface of the Al-25Si specimen.

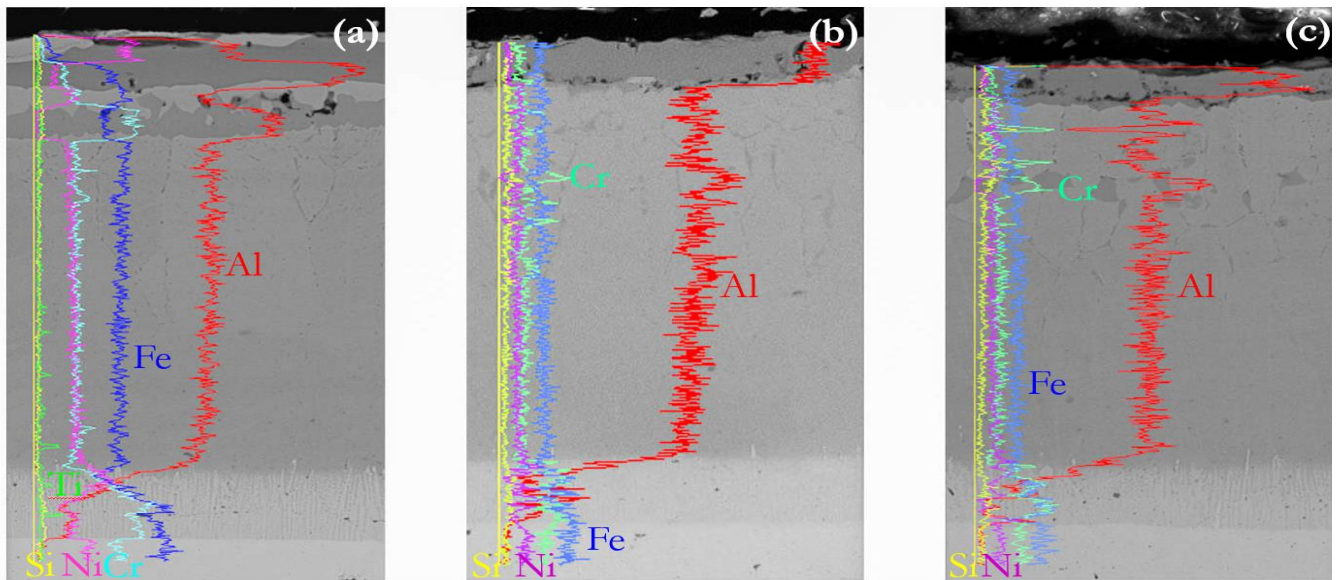


Fig. 6. EDS line scan analysis of (a) Al-12.5Si, (b) Al-25.0Si and (c) Al-37.5Si. (Online-color).

while the IDZ was slightly thicker. The thickness of Al-rich outer layer reduced with greater amount of SiO_2 incorporation in the pack mixture. A total thickness then decreased in the highly doped Al-37.5Si specimen (Fig. 2). These observations are in accordance to the reported results [21]. Therefore, an addition SiO_2 into the pack can decrease the diffusible Al content due to a reduction reaction [21, 22, 24]. Applying the same analysis, XRD patterns at various depths of Al-25.0Si specimen were obtained as Fig 5. The result emphasizes the thickest middle layer was hyperstoichiometric $\beta\text{-(Fe,Ni)Al}$ similar to that of the undoped condition despite the fact that its chemical composition should be assigned as $(\text{Cr,Fe})_5\text{Al}_8$ [14]. The results point out that the formation of aluminide intermetallic coatings of SiO_2 -added pack aluminizing was also governed by predominate Al inward diffusion as similar as the undoped condition discussed earlier.

Regarding to EDS results (Table 3), it was a limited dissolved Si with in aluminides with the concentration less than 5 at.% which is consistent to the phase boundaries of Al-rich Fe_xAl_y intermetallics in Fe-Al-Si and Cr-Al-Si ternary diagrams [33, 34]. This is consistent to the observed Si profiles in the Si co-deposition pack aluminized samples [14, 19, 21]. Since silicide intermetallics was undetected in XRD spectra at various depths (Fig. 4 and Fig.5), it could imply that Si was incorporated in forms of solid solution. High-contrasted regions presented in the thickest middle $\beta\text{-(Fe,Ni)Al}$ layer from the Al-25.0Si and the Al-37.5Si specimens were attributed to segregation of Cr and Si as shown in Fig. 6 This is in good agreement with the EDS point analysis of Spectrum 3 from the Al-25Si specimen. Besides, one may notice that Si is also likely to enrich at the IDZ.

According to the results, it is clearly evident that SiO_2 powder in the mixture can be reduced by Al powder during aluminizing process [21, 22], resulting in the available elemental Si to further react with chloride activator and formed SiH_xCl_y gases. The deposition of Si

into the substrate or aluminide layers by SiH_xCl_y gases is likely to be analogous to pack siliconizing [35, 36]. However, a significant low Si concentration in the aluminides coating might also be due to the relative lower partial pressure of SiH_xCl_y than those of AlCl_x [20, 36, 37]. As the content of SiO_2 in the pack increased, a preferential growth of intermetallics with lower content of Al and a lower Al concentration in the outer layer emphasize that, in this study, a thermodynamic activity of Al can be beneficially suppressed using SiO_2 powder by either a reduction reaction or a change in $\text{SiH}_x\text{Cl}_y:\text{AlCl}_x$. This provides an explanation of a reduction in total thickness of the Al-37.5Si specimen, as also reported in [38].

A growth of the interdiffusion is reported to be controlled by an outward Ni diffusion [19]. In the study, a slight increase in thickness of the Si-containing IDZ layer might indicate an enhancement of Ni diffusion by Si. This correlation is interesting to further.

4. Conclusions

The effect of SiO_2 content for pack aluminized IN800HT were established in this study as follow:

1. The undoped aluminide coatings consisted of 3 main layers: (i) the thickest outer layer consisting of Al-rich Fe_xAl_y compounds, (ii) the middle hyperstoichiometric $\beta\text{-(Fe,Ni)Al}$ and (iii) the inner interdiffusion layer. Cr was rejected from Al-rich Fe_xAl_y compounds because of its limited solubility and formed chromium aluminide $(\text{Cr,Fe})_5\text{Al}_8$ on outer layer and interface between outer layer and middle layer. It is a result of a single step high-activity pack aluminizing as governed by a predominate inward Al diffusion.

2. Addition SiO_2 on a single-step high-activity aluminizing pack cementation process decreased Al in pack mixing and the thermodynamic activity of diffusing Al species, especially for moderate- and high Si specimens.

3. Aluminide coatings from SiO₂-added conditions also composed of three layers where the thickest layer was the middle β -(Fe,Ni)Al layer where the outer layer was diminished.

4. The Al-Si co-deposition in a pack cementation aluminizing using SiO₂ as a silicon source is possible.

5. A limited amount of Si (<5 at.%) was dissolved in aluminides with its segregation observed in separated region in β -(Fe,Ni)Al and the IDZ.

Acknowledgement

Authors are grateful to a materials support from Siam Cement Group (SCG), Thailand. Also, it is gratitude to technical supports and access to a scanning electron microscope in Metallurgy and Materials Science Research Institute (MMRI) and an X-ray diffractometer in Scientific and Technological Research Equipment Centre (STREC), Chulalongkorn University.

References

- [1] G. Chai, J.-O. Nilsson, M. Boström, J. Högberg, and U. Forsberg, "Advanced heat resistant austenitic stainless steels," in *Advanced Steels*. Springer, 2011, pp. 385-397.
- [2] Z.-F. Hu, "Heat-resistant steels, microstructure evolution and life assessment in power plants," in *Thermal Power Plants*. Intechopen, 2012, pp. 195-226.
- [3] D. Zhang, "Introduction to advanced and ultra-supercritical fossil fuel power plants," in *Ultra-Supercritical Coal Power Plants*. Elsevier, 2013, pp. 1-20.
- [4] A. Yamauchi, K. Kurokawa, and H. Takahashi, "Evaporation of Cr₂O₃ in atmospheres containing H₂O," *Oxidation of Metals*, vol. 59, no. (5-6), pp. 517-527, 2003.
- [5] E. J. Opila, "Volatility of common protective oxides in high-temperature water vapor: Current understanding and unanswered questions," *Materials Science Forum*, vol. 461, pp. 765-774, 2004.
- [6] F. Zarei, H. Nuranian, and K. Shirvani, "Effect of Si addition on the microstructure and oxidation behaviour of formed aluminide coating on HH309 steel by cast-aluminizing," *Surface and Coatings Technology*, vol. 394, p. 125901, 2020.
- [7] S. Green and F. Stott, "Aluminizing of iron-nickel-base alloys for resistance to high-temperature gaseous environments," *Corrosion Science*, vol. 33, no. 3, pp. 345-359, 1992.
- [8] R. Dutta, S. Majumdar, A. Laik, K. Singh, U. Kulkarni, I. Sharma, and G. Dey, "Formation and characterization of aluminide coatings on alloy 800 substrate," *Surface and Coatings Technology*, vol. 205, no. 19, pp. 4720-4725, 2011.
- [9] G. Goward and D. Boone, "Mechanisms of formation of diffusion aluminide coatings on nickel-base superalloys," *Oxidation of Metals*, vol. 3, no. 5, pp. 475-495, 1971.
- [10] T. Dudziak, E. Medvedovski, and M. Homa, "Multilayered coatings for high-temperature steam oxidation: TGA studies up to 1000° C," *Journal of Materials Engineering and Performance*, vol. 27, no. 8, pp. 4317-4335, 2018.
- [11] R. Bianco and R. A. Rapp, "Pack cementation diffusion coatings," in *Metallurgical and Ceramic Protective Coatings*. Springer, 1996, pp. 236-260.
- [12] R. Mevrel, C. Duret, and R. Pichoir, "Pack cementation processes," *Materials Science and Technology*, vol. 2, no. 3, pp. 201-206, 1986.
- [13] S. Nikzad, M. Abdi, and S. Rastegari, "Mechanism of Al-Si codeposition on In738LC through single-step diffusion process," *International Journal of Surface Science and Engineering*, vol. 11, no. 1, pp. 1-11, 2017.
- [14] X. Tu, H. Peng, L. Zheng, W. Qi, J. He, H. Guo, and S. Gong, "Oxidation and microstructure evolution of Al-Si coated Ni3Al based single crystal superalloy with high Mo content," *Applied Surface Science*, vol. 325, pp. 20-26, 2015.
- [15] P. Y. Hou, "The reactive element effect—past, present and future," *Materials Science Forum*, vol. 696, pp. 39-44, 2011.
- [16] A. Paúl, R. Sanchez, O. Montes, and J. Odriozola, "The role of silicon in the reactive-elements effect on the oxidation of conventional austenitic stainless steel," *Oxidation of Metals*, vol. 67, no. 1, pp. 87-105, 2007.
- [17] R. Bianco and R. A. Rapp, "Pack cementation aluminide coatings on superalloys: codeposition of Cr and reactive elements," *Journal of the Electrochemical Society*, vol. 140, no. 4, pp. 1181, 1993.
- [18] M. Zandrahimi, J. Vatandoost, and H. Ebrahimifar, "Al, Si, and Al-Si coatings to improve the high-temperature oxidation resistance of AISI 304 stainless steel," *Oxidation of Metals*, vol. 76, no. 3, pp. 347-358, 2011.
- [19] Y. Ruibo, W. Yuxiao, W. Qiong, L. Shusuo, M. Yue, and G. Shengkai, "Microstructure and oxidation behavior of modified aluminide coating on Ni3Al-based single crystal superalloy," *Chinese Journal of Aeronautics*, vol. 25, no. 5, pp. 825-830, 2012.
- [20] R. Bianco, M. A. Harper, and R. A. Rapp, "Codepositing elements by halide-activated pack cementation," *Journal of Materials*, vol. 43, no. 11, pp. 68-73, 1991.
- [21] M. Kim and J. Jung, "Codeposition of Al and Si onto a low carbon steel using silicon dioxide and aluminum and its hot temperature oxidation properties," *Surface and Coatings Technology*, vol. 161, no. (2-3), pp. 218-223, 2002.
- [22] M. Kim, N. Heo, J. Shin, and C. Kim, "Simultaneous chromizing and aluminizing using chromium oxide and aluminum:(I) on low alloy steel," *Surface and Coatings Technology*, vol. 123, no. (2-3), pp. 227-230, 2000.
- [23] M. Hasegawa, "Ellingham diagram," in *Treatise on Process Metallurgy*. Elsevier, 2014, pp. 507-516.

- [24] D. Das, S. Joshi, and V. Singh, "Evolution of aluminide coating microstructure on nickel-base cast superalloy CM-247 in a single-step high-activity aluminizing process," *Metallurgical and Materials Transactions A*, vol. 29, no. (8), pp. 2173-2188, 1998.
- [25] E. Ivanov, "Thermodynamic analysis of phase transformations during aluminizing," *Metallovedenie i Termicheskaya Obrabotka Metallov*, pp. 33-35, 1979.
- [26] D. Pavlyuchkov, B. Przepiórzyński, W. Kowalski, T. Y. Velikanova, and B. Grushko, "Al-Cr-Fe phase diagram. Isothermal Sections in the region above 50 at% Al," *Calphad*, vol. 45, pp. 194-203, 2014.
- [27] P. Budberg, A. Prince, G. Cacciamani, R. Ferro, B. Grushko, P. Perrot, and R. Schmid-Fetzer "Aluminium-iron-nickel," in *Light Metal Systems. Part 2*. SpringerMaterials, 2005, pp. 329-358.
- [28] L. Eleno, K. Frisk, and A. Schneider, "Assessment of the Fe-Ni-Al system," *Intermetallics*, vol. 14, no. (10-11), pp. 1276-1290, 2006.
- [29] I. Chumak, K. W. Richter, and H. Ipsen, "The Fe-Ni-Al phase diagram in the Al-rich (> 50 at.% Al) corner," *Intermetallics*, vol. 15, no. 11, pp. 1416-1424, 2007.
- [30] P. Visuttipitukul, N. Limvanutpong, and P. Wangyao, "Aluminizing of nickel-based superalloys grade in 738 by powder liquid coating," *Materials Transactions*, pp. 1004051047-1004051047, 2010.
- [31] S. Leelachao, V. Thongsiri, and P. Visuttipitukul, "Phase evolution of surface-modified Incoloy 825 superalloy using pack aluminization," *Materials Testing*, vol. 61, no. 9, pp. 829-832, 2019.
- [32] H. Rafiee, H. Arabi, and S. Rastegari, "Effects of temperature and Al-concentration on formation mechanism of an aluminide coating applied on superalloy IN738LC through a single step low activity gas diffusion process," *Journal of Alloys and Compounds*, vol. 505, no. 1, pp. 206-212, 2010.
- [33] V. Raghavan, "Al-Fe-Si (aluminum-iron-silicon)," *Journal of Phase Equilibria*, vol. 15, no. 4, pp. 414-416, 1994.
- [34] Y. Liang, C. Guo, C. Li, and Z. Du, "A thermodynamic description of the Al-Cr-Si system," *Journal of Phase Equilibria and Diffusion*, vol. 30, no. 5, pp. 462-479, 2009.
- [35] J.-K. Yoon, K.-H. Lee, G.-H. Kim, J.-K. Lee, J.-M. Doh, and K.-T. Hong, "Growth kinetics of MoSi₂ coating formed by a pack siliconizing process," *Journal of the Electrochemical Society*, vol. 151, no. 6, p. B309, 2004.
- [36] C. Fu, W. Kong, and G. Cao, "Microstructure and oxidation behavior of Al+ Si co-deposited coatings on nickel-based superalloys," *Surface and Coatings Technology*, vol. 258, pp. 347-352, 2014.
- [37] Z. Xiang and P. Datta, "Codeposition of Al and Si on nickel base superalloys by pack cementation process," *Materials Science and Engineering: A*, vol. 356, no. (1-2), pp. 136-144, 2003.
- [38] A. Eslami, H. Arabi, and S. Rastegari, "Gas phase aluminizing of a nickel base superalloy by a single step HTHA aluminizing process," *Canadian Metallurgical Quarterly*, vol. 48, no. 1, pp. 91-98, 2009.

Appendix

Theoretical ratios of Si/(Si+Al) and the required amount of powders in the pack.

Let us consider the Al is consumed as x mol, the remaining Al is y mol and the obtained Si is z mol. Consider the reduction reaction: $4Al + 3SiO_2 = 3Si + 2Al_2O_3$. It requires Al of 1.33 mol to be used per a mole of the Si obtained,

$$x = 1.33z \quad (1)$$

For all conditions in the study, the content of Al in the pack is constant at 10 g. It is equivalent to 0.3704 mol since an atomic weight of Al is 27 g/mol,

$$x + y = 0.3704 \quad (2)$$

From Eq. (1) and (2), it yields,

$$0.3704 - 1.33z = y \quad (3)$$

As the example, for the Al-12.5Si (Doped Si 12.5at%) condition,

$$z/(y+z) = 0.125 \quad (4)$$

Applying Eq. (3) into Eq. (4), the obtained Si (z) and the remained Al (y) in the pack can be determined based on a basis of 0.3704 mol of Al as follow,

$$z = 0.04457 \text{ mol,}$$

$$y = 0.3111 \text{ mol.}$$

Since a mole of SiO₂ is needed per a mole of Si, an amount of SiO₂ required can be readily calculated by multiplying z with a molecular weight of SiO₂ of 60.08 g/mol; it yields 2.67 g.

Nattapong Nanta, photograph and biography not available at the time of publication.

Patama Visutti pitukul, photograph and biography not available at the time of publication.

Sirichai Leelachao, photograph and biography not available at the time of publication.